Int. J. Electrochem. Sci., 6 **(2011)** 1797 - 1809

International Journal of
ELECTROCHEMICAL
SCIENCE
www.electrochemsci.org

Electrochemical Changes of Pre-Corroded Steel Reinforced Concrete Due to Electrochemical Chloride Extraction

Xiaojian Gao[*], *Yingzi Yang*, *Hongwei Deng*

School of Civil Engineering, Harbin Institute of Technology, P.O.Box 1430, Civil building, 66 West Da-Zhi Street, Harbin 150006, China
[*]E-mail: xjgao2002@yahoo.com.cn

Received: 23 February 2011 / *Accepted:* 4 March 2011 / *Published:* 1 June 2011

This paper presents the electrochemical changes of concrete specimen containing pre-corroded steel rebar with different periods of electrochemical chloride extraction (ECE) treatments. Concrete specimens were prepared with three w/b ratios (0.45, 0.38 and 0.32) and three levels of cement replacement by fly ash at 0%, 10%, 20%. And 3% chloride (NaCl) by mass of binder was added to the mixing water as a source of chloride ions for every mix. The measured electrochemical properties include half-cell potential E_{corr}, corrosion rate I_{corr} and concrete resistivity. The results show that a higher water to cement ratio or more addition of fly ash results in a severer corrosion happening on the reinforcing steel rebar prior to the ECE treatment. Although the resistivity of cover concrete is remarkably improved, the corrosion state is aggravated after ECE treatment according to the E_{corr} and I_{corr} evolution. This worse corrosion state of steel is partly attributed to the temporary alkaline corrosion, confirmed by the highly localized accumulation of alkali (K^+ and Na^+) in the steel-concrete interface and some black-brown corrosion products formed on the steel surface. Therefore, electrochemical chloride extraction (ECE) is capable of removing the chloride ions but is not sufficient to guarantee the repassivation if the corrosion process of steel has already occurred.

Keywords: Steel corrosion, electrochemical chloride extraction, electrochemical property, alkaline corrosion, repassivation

1. INTRODUCTION

Steel-reinforced concrete has been extensively used as a structural material for many years because of its low cost, ease of construction and good durability. However, with exposure to chloride ions, the steel embedded in concrete may corrode and form expansive products at the steel/concrete interface, causing cracking and spalling of concrete cover and reducing its service life [1-2]. The conventional way of restoration of reinforced concrete structures consists of removing the outer

chloride-contaminated concrete layer and corroded steel rebar and replacing them by new, alkaline mortar or concrete and intact reinforcement. This method has many disadvantages such as the environment effects (noise, dust, concrete waste, etc.), the difficulty of effectively removing chlorides from the interior concrete of the structure and very high direct costs (repair work and material) as well as indirect costs (traffic jam, waiting times, etc.) [3]. Alternative techniques such as electrochemical chloride extraction (ECE) have thus been developed and applied [4]. ECE technique normally use an impressed current that transforms the steel rebar from a collection of anodic and cathodic sites to a cathode with the addition of an external electrode and power supply to the surface of the concrete [4,5]. The resultant electrical field gradient repulses the negative chloride ions and other anions away from the reinforcing steel. ECE has proven to be a nearly non-destructive and cost effective rehabilitation technique for chloride-contaminated reinforced concrete structures [6], although it could induce some undesirable side-effects such as hydrogen evolution, the risk of accelerated alkali-silica reaction for some type of aggregates and the risk of increased porosity of the concrete near the interface [7-8].

The chloride removal efficiency of ECE treatment has been fully discussed in previous researches in which many factors such as different electrolytes, anode type and arrangement, current densities, treatment durations, specimen shapes, reinforcement arrangement and various cements were considered [9-16]. However, less work has been done on the subsequent electrochemical behavior of the steel-concrete system after ECE treatment [17-18] and the resulting repassivation probability and corrosion rate are highly questionable [19-20]. On one hand, the half-cell potential mappings performed on field structures showed that the reinforcement was completely repassivated after the ECE treatment and remained in fully passive condition for nearly 20 years when further chloride ingress was avoided by application of a coating [19]. Based on the lab study, Glass and Buenfeld [21] reported that the formation of a $Ca(OH)_2$ layer on the surface steel increases its tolerance to chlorides and limits the corrosion rate of reinforcement. On the other hand, visual observations revealed no significant changes happened when the ECE treatment was applied [5]. Using linear polarization resistance techniques, Green et al. [18] concluded that the ECE treatment did not significantly reduce the corrosion rate of steel. And ECE is considered to be capable of removing the chloride but not halt the damage when the process of corrosion is advanced [20].

It is the intention of this work to present electrochemical properties, including hall-cell potential, corrosion rate and concrete resistivity, of the pre-corroded steel-concrete system before and after ECE treatment and the microstructure changes of the steel-concrete interface, so that a more detailed understanding of the corrosion state and future durability of treated structures can be achieved.

2. EXPERIMENTAL MATERIALS AND METHODS

2.1. Materials

As shown in Table 1, five concrete mixes were prepared with three w/b ratios (0.45, 0.38 and 0.32) and three levels of cement replacement by fly ash at 0%, 10%, 20% (when w/b ratio was

maintained constant at 0.32). The constituents of mixes included: Ordinary Portland cement with strength grade of 42.5 according to Chinese standard GB175-2007, grade Ⅱ fly ash with a water requirement ratio of 97% according to Chinese Standard GB1596-2005, natural river sand with a fineness modulus of 2.82 and continuously graded crushed granite gravel with a maximum size of 25 mm and crushed index of 4.8%. At the same time, a commercially available, naphthalene-based, superplasticizer (SP) was used with different level of dosage in each mix to improve the workability of fresh concrete (with slump of 180±10 mm), resulting in a good compaction for every specimen. For every mix, 3% chloride (NaCl) by mass of binder was added to the mixing water as a source of chloride ions. Tap water was used for mixing and curing of concrete specimens.

Clean steel rods of 10 mm diameter and 150 mm height were used in specimens as reinforcement, which were recently pickled in a 50% citric acid solution, cleaned in distilled water and immediately dried with compressed air. A titanium mesh having an electrical resistivity of 5.6×10^{-5} Ω cm was used as the anode and saturated calcium hydroxide ($Ca(OH)_2$) solution was used as the electrolyte in ECE treatment.

Table 1. Mixing proportion of concrete（kg/m^3）

No.	w/b	Cement	Water	Fly ash	Sand	Gravel	SP	NaCl
0.45	0.45	480	216	0	613	1091	0.5	14.4
0.38	0.38	480	182	0	626	1112	1.5	14.4
0.32(OPC)	0.32	480	154	0	636	1130	3.12	14.4
FA10	0.32	432	154	48	636	1130	3.12	14.4
FA20	0.32	384	154	96	636	1130	3.0	14.4

2.2. Experimental methods

Cylindrical concrete specimens of 100 mm diameter and 150 mm height were cast and a steel rod was placed in the axial direction with an embedded length of 100 mm as shown in Fig. 1. Immediately after casting, the specimens were cured in a moist cabinet for 24 h, removed from the moulds, wrapped with the plastic sheets and cured for 27 days at room temperature (20±2℃). After curing, all specimens were immersed in the saturated $Ca(OH)_2$ solution for 24 h in order to saturate the specimen, reduce the initial electrical resistance and facilitate the ECE process. Then, the saturated specimens were connected to the DC power supply with voltage of ~ 60V to perform the ECE process as shown in Fig. 2.

The adjustable resistor was reset once a day to keep a constant current density of 2.0 A/m^2 of steel surface applied in the ECE process. The chloride ion concentration and pH value of the electrolyte were detected everyday and the $Ca(OH)_2$ solution was renewed every two days. The treatment periods were 7, 14, 21 and 28 days.

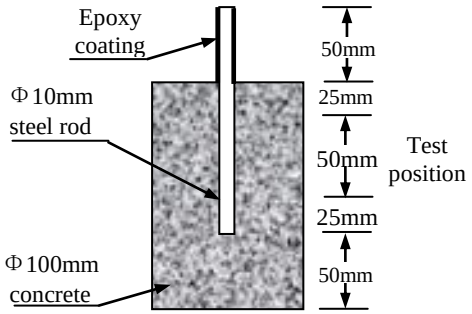

Figure 1. concrete specimen for ECE treatment

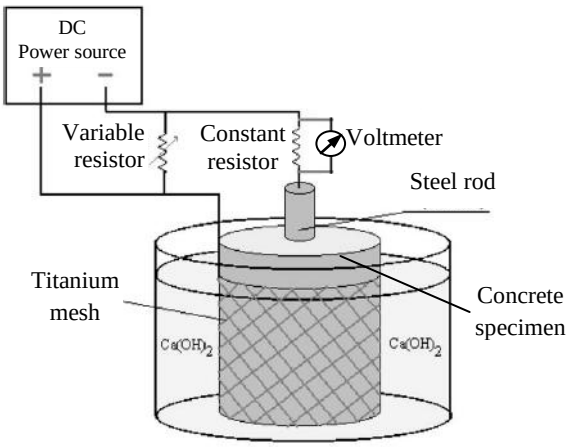

Figure 2. Experimental ECE set-up.

Electrochemical measurements were conducted immediately after each ECE period. Two specimens were tested each time. The corrosion state of steel rod was evaluated by two electrochemical parameters: the half-cell potential (E_{corr}) versus a saturated calomel electrode (SCE) and the corrosion rate (I_{corr}) determined by the linear polarization resistance technology [22]. A three-electrode method was used in the linear polarization resistance test. The steel rod was cathodically and anodically polarized 20 mV from the half-cell potential using a sweep rate of 12mV/min. This sweep is recommended by Gonzalez et al. [23]. On the other hand, the electrical resistivity of cover concrete was also measured for every specimen using the Wenner four-probe method [24].

After the completion of 28 days ECE treatment, the specimen was longitudinally split into two half parts to observe the steel surface condition and mortar samples were selected from the steel nearby zones (2~3 mm depth) for investigation of free chloride and alkaline ion contents and microstructure. The dried mortar sample was ground to pass through 80-μm sieve, placed into distilled water with a know volume, and concentrations of free chloride ion, potassium and sodium ions in the solution were detected. A JEOL SX-4 scanning electron microscope (SEM) was used for observing selected samples and the accelerating voltage was maintained at 20 kV. Samples were coated with a thin film of gold before testing. The elemental micro-analyses were identified by an energy dispersive X-ray

spectroscopy (EDS) coupled with the SEM system. The resolution power of EDX is 129.92 eV and the testing time is set to 50 s.

3. RESULTS AND DISCUSSION

3.1 Half-cell potential

Half-cell potential measurement has been widely used to assess the likelihood of corrosion of reinforcing rebar in concrete structures. The half-cell potential represents the thermodynamic trend of corrosion, but it cannot be used to represent the instantaneous corrosion rate. As the reinforcing bar changes from a passive to an active state the potential of the steel measured against a reference electrode becomes increasingly more negative. It is suggested in ASTM C-876 (as shown in Table 2) that, the rebar has a corrosion possibility higher than 90% when the measured half-cell potential is lower than −278 mV (SCE) and a potential lower than −426 mV (SCE) represents a severe corrosion happened on the steel [22].

Table 2. Corrosion risk from potential measurement according to ASTM C876 [22]

Potential (vs. SCE) / mV	Probable corrosion rate
＞-128	Low (10% corrosion risk)
-128 to -278	Intermediate corrosion risk
＜-278	High (90% corrosion risk)
＜-426	Severe corrosion

Figure 3 presents the half-cell potential change of the steel rod before and after ECE treatment. It can be found that all the potentials were lower than −426 mV before ECE treatment, indicating that the passive layer breakdown and severe corrosion happened in every specimen. Such terrible pre-corrosion state of steel rebar is attributed to the addition of 3% NaCl into concrete mixture, which is much higher than the threshold chloride content for corrosion of steel in concrete [25-26]. Both a higher w/b ratio and a more cement replacement by fly ash resulted in a lower half-cell potential being attributed to a higher porosity and easier oxygen transport in concrete at early ages. It was also reported that the partial cement replacement by fly ash had invisible influence on the half-cell potential of steel in concrete when immersed in chloride solution [27]. Even the addition of fly ash showed a reduced corrosion level in some cases, which was explained by the higher content of Al_2O_3 in fly ash to form more chloroaluminate (Friedel salt) [28]. However, the tested specimens in those experiments experienced more than 28 days curing which was favorable for the pozzolanic reaction of fly ash.

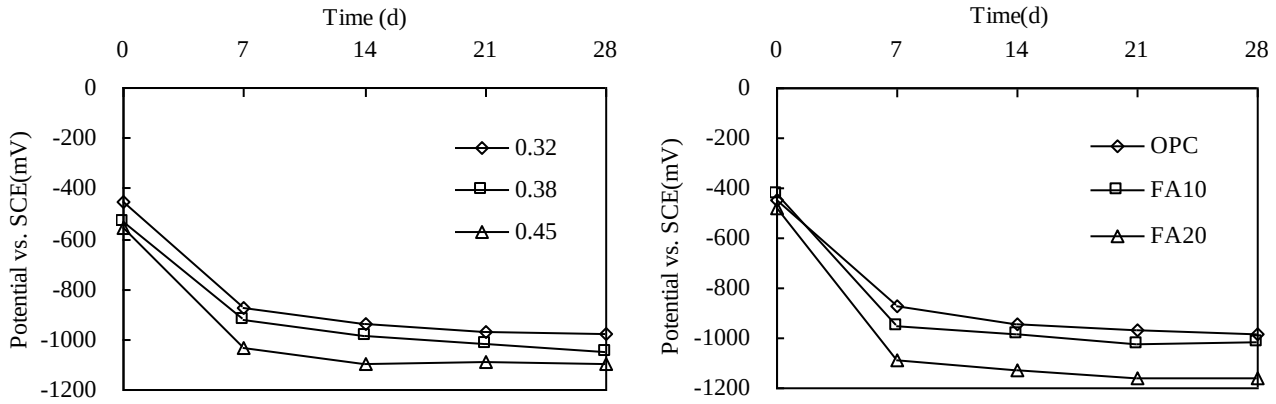

(a) Different w/c ratio (b) Different fly ash addition

Figure 3. Half-cell potential evolution of the steel with the ECE treatment time

After 7 days of ECE treatment, the potential readings abruptly decreased to -870~-1090 mV from −430~−550 mV prior to the treatment, and then they developed slowly with the treatment period to more negative readings of -980~-1160 mV until 28 days. Garcés [13] found that the half-cell potential decreased to -600~-700 mV (versus $Cu/CuSO_4$ saturated reference electrode) at the end of ECE treatment and even became more negative during the following 3 years. Elsener and Fajardo [29-30] reported that the potentials of the steel were as negative as -1000 mV during the ECE treatment and moved toward the same levels or even more positive values than those before the treatment. Other authors [13, 15] suggested that a depolarization process was necessary to get a more meaningful potential result for ECE treated samples. Therefore, the E_{corr} values in this study, being more and more negative from the beginning to the end of ECE treatment, is alone not enough to evaluate the corrosion state of steel.

3.2. Corrosion current density

In order to quantify the instantaneous corrosion state of steel, the electrochemical measurement of corrosion rate was carried out by the polarization resistance method [31]. It was well-known that this method contains an ohmic drop effect due to the resistance change of concrete. However, modern potentiostats enable compensation for the ohmic drop through the concrete between the steel and the reference electrode [22]. According to a previous study [32], four ranges of the corrosion rate are proposed as presented in Table 3. When the corrosion current density is within 0.1 to 0.5μA/cm^2, the corrosion rate is slow. When the corrosion current density is within 0.5 to 1 μA/cm^2, the corrosion rate is mediated.

The measurement results of corrosion current densities are presented in Fig. 4. It was found that the corrosion rate for concrete specimens prior to ECE treatment ranged from 0.2 to 0.3μA/cm^2, then it is concluded that every sample encountered a low to moderate level of corrosion due to the addition of

chloride. When a higher water to cement ratio or more addition of fly ash was adopted in concrete mix, a higher current density was detected during the test which representing a worse corrosion state.

Table 3. Corrosion rate and level of corrosion [32]

Corrosion rate i_{corr} (μA/cm^2)	Corrosion level
< 0.1	Passive/negligible
0.1~0.5	Low to moderate
0.5~1.0	Moderate to high
> 1.0	High

This tendency accords with what was presented by potential readings in Part 3.1. The ECE treated samples showed much higher corrosion rates than those prior to the treatment, and a longer treatment time led to a more increase in corrosion rate. After the completion of 28 days chloride extraction, the corrosion rate increased to 1.5 to 2.0 times of the initial value for every sample. For those two specimens with high water to cement ratios (0.38 and 0.45), the corrosion rates changed into the moderate to high level (beyond 0.5μA/cm^2) after the ECE treatment. Several researchers found that the ECE treatment markedly decreased the corrosion rates of steel, but the remained values of I_{corr} were still higher than the limit of 0.1μA/cm^2 proposed for passive conditions [14, 29]. On the other hand, other works found corrosion rates of steel became higher than before the ECE treatment [18, 33]. The same finding was demonstrated by the electrochemical measurements in this study.

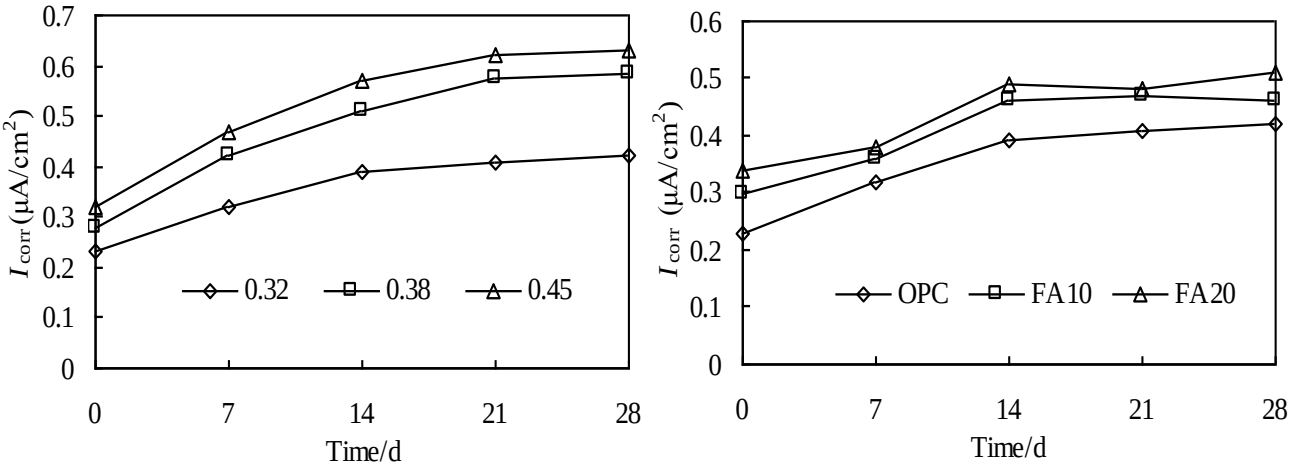

(a) Different w/c ratio (b) Different fly ash addition

Figure 4. I_{corr} evolution of the steel with the ECE treatment time

3.3. Concrete resistivity

Once depassified, the electrical resistivity of the concrete cover and oxygen transport are both controlling factors for the corrosion rate of reinforcement. Wenner's four-probe resistivity measurements were performed on the specimens before and after different periods of ECE treatment [34]. It should be noticed that the water content inside the concrete affects the resistivity. In this study, a SSD (saturated, surface dried) condition of concrete is ensured for every test. In a similar fashion to half-cell potential, concrete resistivity in the zone of corrosion activity provides information on the general corrosion risk [35-36], as shown in Table 4.

Table 4. Empirical resistivity thresholds for depassivated steel

Resistivity (kΩ-cm)	Probable corrosion rate
< 5	Very high
5~10	High
10~20	Low to moderate
> 20	Low/negligible

Figure 5 presents the resistivity values of the cover concrete for each specimen before and after the ECE treatment. It can be found that every specimen showed a low resistivity value ranging from 5 to 10 kΩ-cm before ECE treatment, being attributable to the high concentration of free chlorides containing in concrete mix.

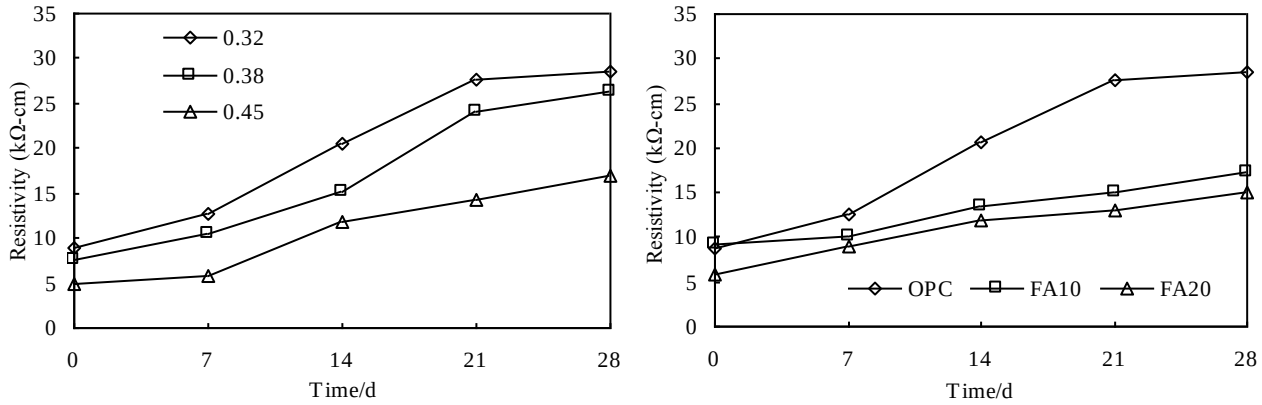

(a) Different w/c ratio (b) Different fly ash addition

Figure 5. The evolution of the cover concrete resistivity with the ECE treatment time

This deficiency in concrete resistivity partly led to the passive layer breakdown and severe corrosion state as demonstrated by the E_{corr} and I_{corr} results. As expected, the concrete resistivity

decreased with the increasing of water to cement ratio. The addition of 10% fly ash has no visible influence on the initial resistivity due to its good particle compaction effects in cement paste, but the higher addition of fly ash (20%) shows a lower resistivity due to its lower pozzolanic reactivity at early ages [37]. During the ECE treatment, the concrete resistivity increased very quickly and developed to more than three times of the initial value until 28 days treatment for every sample without fly ash. However, a much slower increase of resistivity was observed for concretes containing fly ash, which can be explained as the result of impurities like unburnt carbon introduced by fly ash [38]. In any case, the increased concrete resistivity is mainly due to the reduction of free chloride in concrete [15], which means a better protection against the further corrosion of reinforcement.

3.4. Alkali ions accumulation and microstructure observation

Table 5 presents the content of Na^+ and K^+ ions in the steel/concrete interface for every specimen. It can be seen that prior to treatment, the Na^+ ion content was as high as about 7 kg per m^3 of concrete due to the addition of NaCl during mixing. The K^+ ion was mainly from the cement and its content was reduced by the addition of fly ash to replace cement. After ECE treatment, a much higher content of Na^+, 24~29 kg per m^3 of concrete which was about 3 to 4 times of the initial value, was found near the steel surface as expected. The content of K^+ ions became doubled after the ECE treatment, and the less increase content for K^+ ion than for Na^+ ions may be related to the lower initial content. This accumulation tendency of alkali ions in the steel surface was aggravated by the increasing water to cement ratio and the more addition of fly ash, indicating the increased negative effects on long-term performance of structures [5, 39].

Table 5. Content of alkaline ions in the steel/mortar interface (within 2-3 mm) before and after ECE treatment

Concrete	Potassium ions (kg/m^3)		Sodium ions(kg/m^3)	
	Before	After	Before	After
0.45	1.69	3.51	7.06	29.32
0.38	1.78	3.38	7.15	27.73
0.32	1.80	3.25	7.21	24.47
FA10	1.76	3.31	7.07	24.91
FA20	1.68	3.42	6.95	25.50

After the ECE treatment, there was not so much mortar adhering to the surface of steel in concrete specimen, instead, some white substance was found covering the surface of all steel samples and filling the steel-concrete interface zone as shown in Fig. 6. Such white deposit on the steel surface was also found by other researchers [5, 39], being attributable to the accumulation of alkali ions and

$Ca(OH)_2$. On the other hand, all steel samples had large areas that were discolored black-brown showing very severe corrosion occurred on the steel.

Figure 7 and Figure 8 show the microstructure and elemental micro-analysis of mortar samples nearby the steel after ECE treatment. The typical C-S-H phase with a characteristic of reticulated morphology was hardly observed and the mortar had a very open microstructure with a high porosity, such degradation tendency was also observed in previous studies [5, 40]. A few of hexagonal calcium hydroxide crystals with huge size formed in the mortar as shown in Fig. 7.

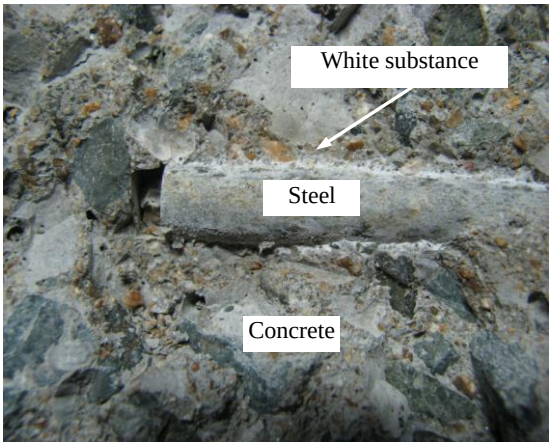

Figure 6. Abundant white substance forms in the steel-concrete interface zone

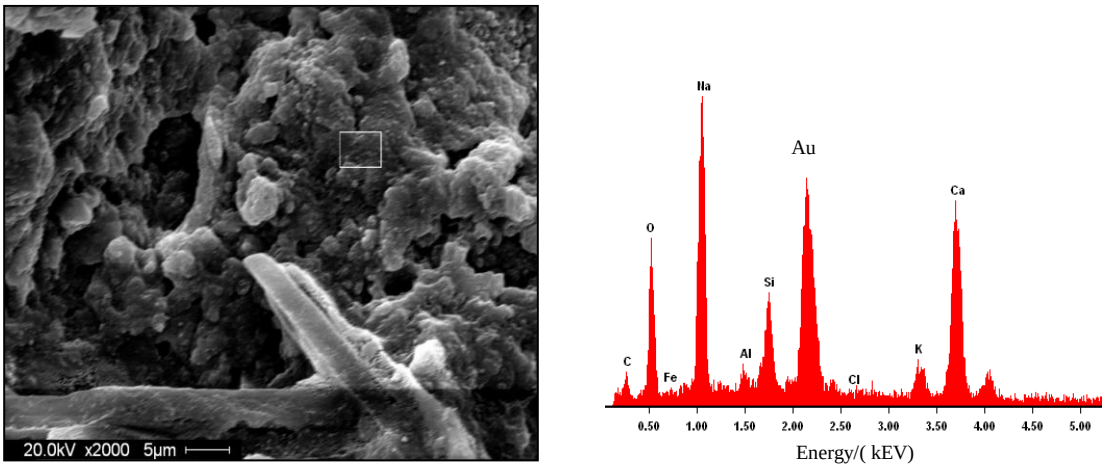

Figure 7. A great deal of spherulite and sodium-calcium-rich crystals formed instead of CSH phases in the mortar nearby the rebar

An accumulation of fine spherulite (in Fig.7) and flaky (in Fig.8) crystals was detected in the samples and they were demonstrated to be sodium-calcium-rich by EDS analysis. Such microstructure characteristic exactly accords with the results of Na^+ and K^+ ion accumulation and the observed degradation of the steel-concrete interface zone.

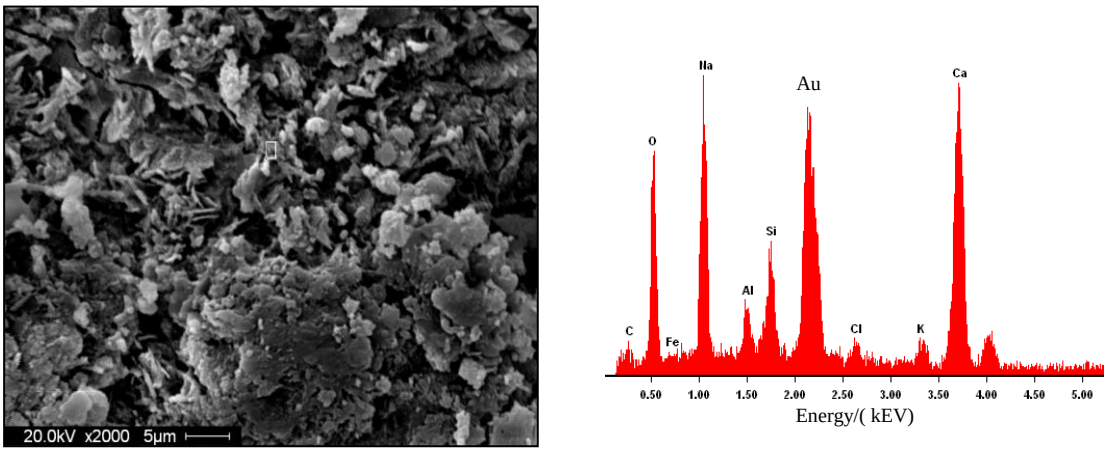

Figure 8. A mass of fine plate-like and sodium-calcium-rich crystals formed instead of CSH phases in the mortar nearby the rebar

3.5. Discussion

From the half-cell potential and corrosion rate measurements reported in Section 3.1 and 3.2, it can be clearly verified that all the rebar samples became depassivated and underwent a moderate or even severe level of corrosion induced by the introduction of chloride ions prior to the ECE treatment. Both a higher water to cement ratio and a more addition of fly ash (20%) lead to a lower half-cell potential and higher corrosion rate indicating a worse corrosion, being attributable to an increased porosity in concrete which has been proven by the concrete resistivity results.

Under the external electric field of ECE treatment, most of free chloride ions are expelled from the concrete and dissolved into the outer electrolyte [30], therefore, the concrete resistivity is increased to a higher level which indicating a better protection against corrosion of reinforcement. Unfortunately, the measured half-cell potential and corrosion current density showed an evidently severer corrosion happening to the embedded rebar during the ECE treatment, in contradiction to the reduced content of free chloride ions in concrete.

The more negative potential is partly due to the strong cathodic polarization exerted by the ECE treatment, and corrosion measurements are suggested after an extended time period of depolarization that depends on the rate of oxygen arrival at the rebar (repassivation) [13, 15]. However, the several times increased concentration of alkaline ions with degrading C-S-H phase and the discolored black-brown corrosion products observed on the surface of rebar support further the possibility of a temporary alkaline attack on the pre-corroded steel. This is due to two factors. First, the treatment reduced any passive film along with any existing corrosion products on the surface of the steel leaving it susceptible to active general corrosion over the whole steel area. It also electrochemically reduced any dissolved oxygen in the local concrete pore solution, thereby eliminating any possibility of repassivation. Second, the treatment resulted in a localized accumulation of alkali (K^+ and Na^+) and hydroxide ions because of ion migration and water hydrolysis at the steel

surface [15, 29], increasing the pH to very high levels and putting the steel in the alkaline corrosion region of the E/pH diagram [17]. Similar results have been observed by other researchers [33]. Therefore, the ECE treatment reduces chloride-induced corrosion due to chloride extraction but increases the overall general corrosion rate due to the alkaline corrosion when the steel is pre-corroded.

Several authors reported that the corrosion rate decreased with the time after the completion of ECE treatment [13-14], and the corrosion rate measured shortly after the treatment completion was likely to have overestimated the equilibrium corrosion rate. However, the final corrosion rates in those experiments still remained higher than the limit for passive conditions after several months, indicating that only ECE treatment is incapable of restoring deteriorated structures to their original state, i.e. the passive state. To improve the repassivating efficiency of ECE treatment, it was suggested that both the ECE treatment and migration of calcium nitrite were simultaneously applied to reinforced concrete structures [41]. To fully understand this new technology, further studies should be done in this field.

4. CONCLUSIONS

The following conclusions can be drawn from the above investigation:

- With the same amount of chloride added in concrete mix, a higher water to cement ratio or more addition of fly ash results in a severer corrosion happening on the reinforcing steel rebar prior to the ECE treatment.
- Although the resistivity of cover concrete showed a remarkable increase due to the reduction of free chloride ions after ECE treatment, the more negative E_{corr} values and increased I_{corr} values were detected, indicating an aggravated corrosion on the steel.
- The highly localized accumulation of alkali (K^+ and Na^+) was detected in the steel-concrete interface and some black-brown corrosion products formed on the steel surface after the ECE treatment. Therefore, the aggravated corrosion state of steel after ECE treatment was partly attributed to the temporary alkaline corrosion.
- Electrochemical chloride extraction (ECE) is capable of removing the chloride ions but is not sufficient to halt the corrosion if the process of deterioration has already occurred. Future works are required to determine the limit of corrosion state for which steel repassivation is still possible and new technologies are needed to improve the ECE efficiency.

ACKNOWLEDGEMENTS
This work is funded by the National Natural Science Foundation of China (No. 50878086) and Specialized Research Fund for the Doctoral Program of Higher Education (No. 20070213036).

References

1. P. K. Mehta, *Concrete in the Marine Environment*, Elsevier Applied Science, New York (1991)
2. L. T. N. Dao, V. T. N. Dao, S. H. Kim and K. Y. Ann, *Int. J. Electrochem. Sci.*, 5 (2010) 302.

3. A.Sharif, M. K. Rahman, A. S. Al-Gahtani, M. Hameeduddin, *Cem. Concr. Compos.*, 28 (2006) 734.
4. B. Elsener, M. Molina and H. Böhni, *Corrosion Sci.*, 35 (1993) 1563.
5. N. R. Buenfeld, J. P. Broomfield, *Mag. Concr. Res.*, 52 (2000) 79.
6. J. C. Orellan, G. Escadeillas, G. Arliguie, *Cem. Concr. Res.*, 34 (2004) 227.
7. M. Siegwart, J. F. Lyness, B. J. McFarland, G. Doyle, *Constr. Build. Mater.*, 19 (2005) 585.
8. M. Siegwart, J. F. Lyness, B. J. McFarland, *Cem. Concr. Res.*, 33 (2003) 1211.
9. R. B. Polder, *Constr. Build. Mater.*, 10 (1996) 83.
10. C. Arya, P.Vassie, *Cem. Concr. Res.*, 26 (1996) 851.
11. A.Toumi, R. Francois, O. Alvarado, *Cem. Concr. Res.*, 37 (2007) 54.
12. M. I. Nzeribe, B. H. Brian, M. H. Carolyn, *Cem. Concr. Res.*, 26 (1996) 165.
13. P. Garcés, M. J. Sánchez de Rojas, M. A. Climent, *Corrosion Sci.*, 48 (2006) 531.
14. J. C. Orellan Herrera, G. Escadeillas, G. Arliguie, *Cem. Concr. Res.*, 36 (2006) 1939.
15. W. Yeih, J. J. Chang, C. C. Hung, *Cem. Concr. Res.*, 36 (2006) 562.
16. A.C. Miguel, J. S. María, V. Guillem, *ACI Mater. J.*, 103 (2006) 243.
17. T. D. Marcotte, C. M. Hansson, B. B. Hope, *Cem. Concr. Res.*, 29 (1999) 1555.
18. W. K. Green, S. B. Lyon, J. D. Scantlebury, *Corrosion Sci.*, 35 (1993) 1627.
19. B. Elsener, *Mate. Corros.*, 59 (2008) 91.
20. J. M. Miranda, A. Cobo, E. Otero, J. A. González, *Cem. Concr. Res.*, 37 (2007) 596.
21. G. K. Glass, N. R. Buenfeld, *Corrosion Sci.*, 42 (2000) 923.
22. M. W. John, V. Øystein, *Constr. Build. Mater.*, 18 (2004) 351.
23. J. Gonzalez, A. Molina, M. Escudero, C. Andrade, *Corrosion Sci.*, 25 (1985) 917.
24. K. R. Gowers, S. G. Millard, *ACI Mater. J.*, 96 (1999) 536.
25. S. E. Hussain, A. S. Al-Gahtani, Rasheeduzzafar, *ACI Mater. J.*, 93 (1996) 534.
26. M. Thomas, *Cem. Concr. Res.*, 26 (1996) 513.
27. Y. S. Choi, J. G. Kim, K. M. Lee, *Corrosion Sci.*, 48 (2006) 1733.
28. S. P. Arredondo-Rea, R. Corral-Higuera, M. A. Neri-Flores, J. M. Gómez-Soberón, F. Almeraya-Calderón, J. H. Castorena-González, J. L. Almaral-Sánchez, *Int. J. Electrochem. Sci.*, 6 (2011) 475.
29. G. Fajardo, G. Escadeillas, G. Arliguie, *Corrosion Sci.*, 48 (2006) 110.
30. B. Elsener, U. Angst, *Corrosion Sci.*, 49 (2007) 4504.
31. M. A. Ameer, A. M. Fekry, A. A. Ghoneim, F. A. Attaby, *Int. J. Electrochem. Sci.*, 5 (2010) 1847.
32. C. Andrade, C. Alonso, *Constr. Build. Mater.*, 15 (2001) 141.
33. C. Andrade, M. Castellote, J. Sarria, C. Alonso, *Mater. Struct.*, 32 (1999) 427.
34. W. Morris, E. I. Moreno, A. A. Sagüés, *Cem. Concr. Res.*, 26 (1996) 1779.
35. W. Lopez, J. A. Gonzalez, *Cem. Concr. Res.*, 23 (1993) 368.
36. J. P. Broomfield, *Corrosion of steel in concrete*, E&FN Spon, London (1997)
37. R. B. Polder, W. H. A. Peelen, *Cem. Concr. Compos.*, 24 (2002) 427.
38. V. Saraswathy, S. Muralidharan, K. Thangavel, S. Srinivasan, *Cem. Concr. Compos.*, 25 (2003) 673.
39. N. M. Inekwaba, B. B. Hope, C. M. Hansson, *Cem. Concr. Res.*, 26 (1996) 267.
40. T. D. Marcotte, C. M. Hansson, B. B. Hope, *Cem. Concr. Res.*, 29 (1999) 1561.
41. M. Sánchez, M. C. Alonso, *Constr. Build. Mater.*, 25 (2011) 873.

© 2011 by ESG (www.electrochemsci.org)